

Deep Resolve: Unrivaled Speed in MRI

Nicolas Behl, Ph.D.

Global Marketing Manager MRI Systems, Siemens Healthineers, Erlangen, Germany

How artificial intelligence is changing imaging

The rapid advancement of artificial intelligence (AI), particularly in the realm of deep learning, is transforming image reconstruction. Neural networks trained on vast datasets are reshaping how we reconstruct and enhance images. This transformation is greatly facilitated by increased access to powerful computing resources, such as high-performance graphics processing units (GPU). The continued evolution of this field and the synergy between deep learning and image reconstruction is creating unique opportunities for augmenting innovation and precision.

Deep Resolve: Shaping the next generation of MRI

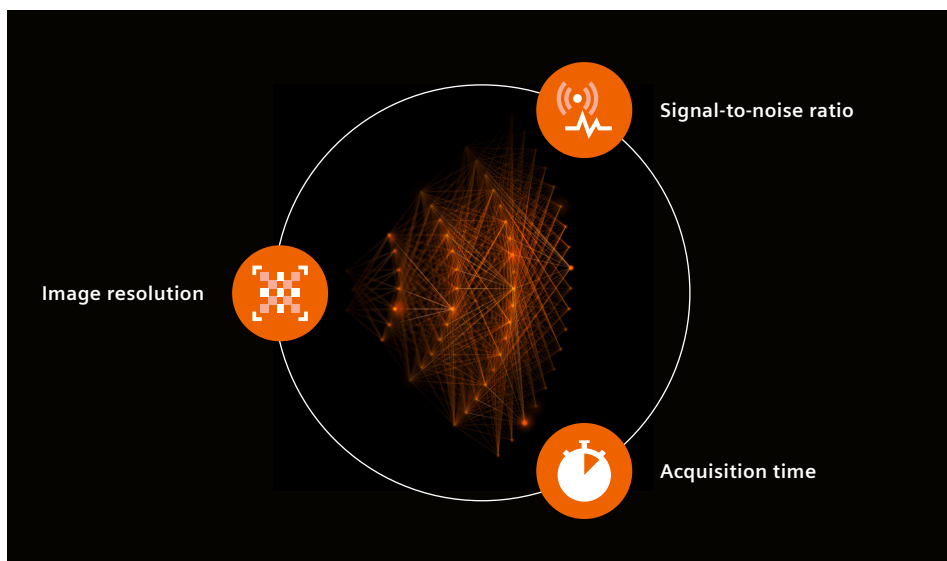
Deep Resolve is an AI-powered image reconstruction technology that is altering the way we approach magnetic resonance imaging (MRI). It can significantly reduce acquisition times while simultaneously improving image sharpness, even in small structures. It bypasses the compromises that

come with conventional acceleration methods such as parallel imaging, and directly targets the main limitations of MRI: signal-to-noise ratio (SNR), image resolution, and acquisition speed (Fig. 1).

Deep Resolve can help alleviate the burden on health-care systems by reducing waiting times for MRI exams, and it can extend MRI to patients who cannot tolerate long scans. It can also create more flexibility for adding acquisitions that would otherwise be omitted due to time constraints.

The technologies within Deep Resolve

Deep Resolve contains the AI powered image reconstruction technologies Deep Resolve Boost, which addresses image noise introduced by high acceleration factors and Deep Resolve Sharp, which increases the sharpness and resolution of an MR image. Alternatively, Deep Resolve Gain can be used for noise reduction instead of Deep Resolve Boost (Fig. 2). In the following, we will describe how each of the technologies work and what the benefits are.



1 Image resolution, signal-to-noise ratio, and acquisition time are the three defining factors in MRI. Using conventional methods, changing one of them affects at least one of the other two. Deep learning reconstruction has the potential to overcome this.

Deep Resolve Gain

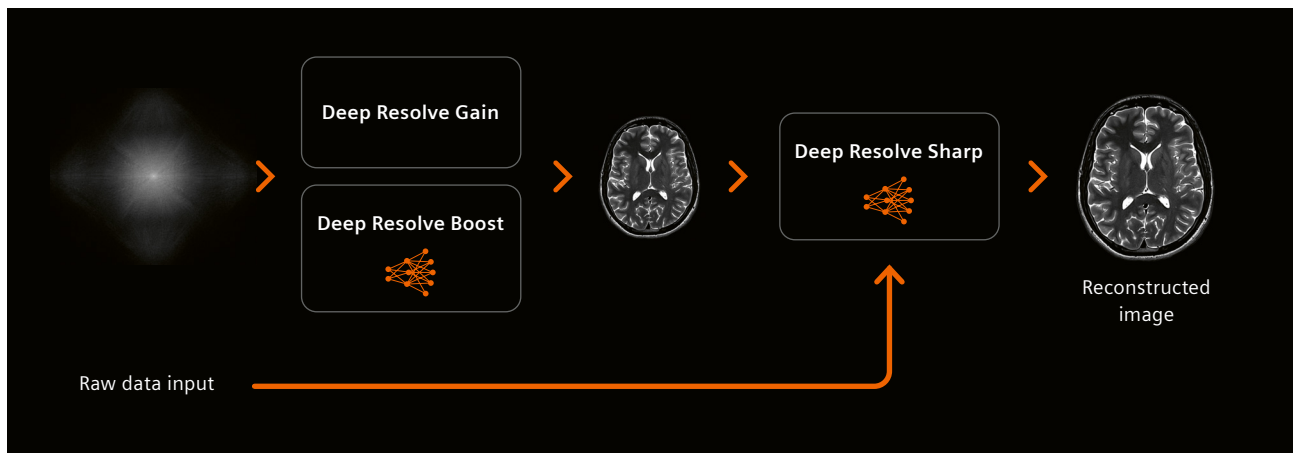
Deep Resolve Gain tackles a common problem in MRI: image noise. Traditional noise filters operate globally on the entire reconstructed image and cannot account for local variations in noise that may be caused by MRI coil array geometries, patient variability, or parallel imaging reconstruction techniques. Deep Resolve Gain uses noise maps generated from the original raw data to address this issue. This targeted denoising improves the SNR and image quality without extending acquisition time (Fig. 3).

Deep Resolve Gain uses the acquired MRI data to generate a noise map that reflects spatial noise variations. This noise map is then incorporated directly into the image denoising process, addressing the local variations in image noise that cannot be addressed by conventional noise filters. The denoising algorithm takes local noise variations into account and enables stronger denoising where noise would be most dominant, resulting in images that have a higher SNR.

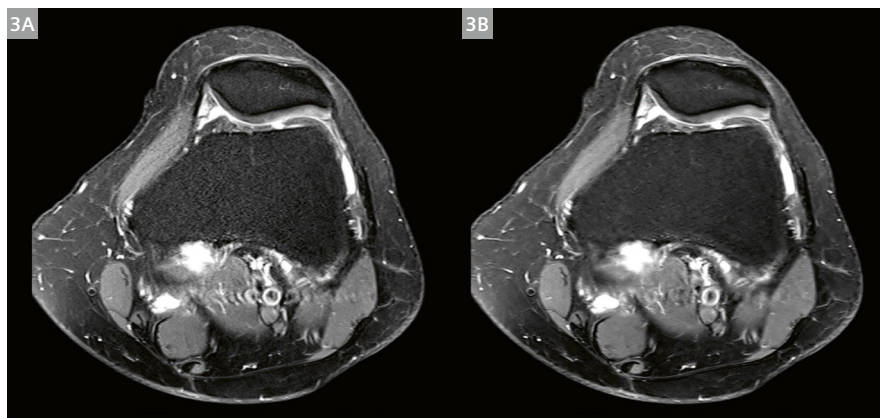
The technology behind Deep Resolve Gain uses individual noise maps as input for an iterative reconstruction process, similar to the one used in Compressed Sensing. However, Deep Resolve Gain extends this process to Cartesian 2D imaging and performs denoising in the wavelet domain. This is more efficient than denoising in the image or frequency domain, and enables better separation between noise and small structures that are part of the image to be reconstructed. Moreover, the denoising strength of Deep Resolve Gain can be adjusted to suit the amount of noise, as well as personal preferences.

Deep Resolve Boost

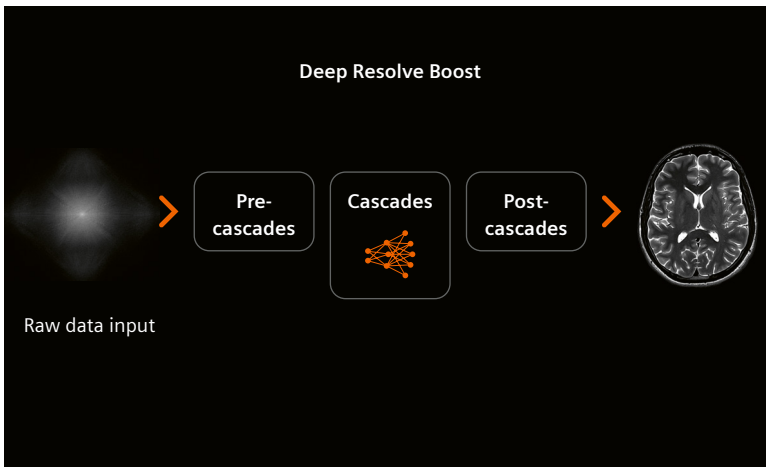
Deep Resolve Boost enables high acceleration without sacrificing SNR. As a raw-data-to-image deep learning reconstruction technology, it leverages the availability of raw data throughout the reconstruction, delivering excellent performance and robust results.



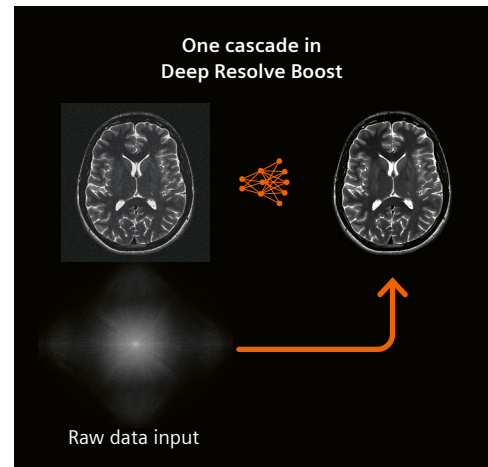
2 The reconstruction process with Deep Resolve usually consists of two steps. In the first step a denoising method, either Deep Resolve Gain or Deep Resolve Boost, is applied to generate a high-SNR output using data originating from an accelerated acquisition as input. Then, Deep Resolve Sharp is employed to further increase image sharpness and resolution.



3 Reconstructions of a PD TSE fs acquisition of the knee with a PAT factor of 3 on a 3T MAGNETOM Vida. **(3A)** The conventional reconstruction is affected by noise due to the high acceleration factor. **(3B)** The reconstruction with Deep Resolve Gain markedly reduces the noise without sacrificing details in the image.



4 During the reconstruction process with Deep Resolve Boost, the raw data is processed through three different types of cascades. The pre-cascades are employed to generate an initial estimate of the reconstructed image. Within the actual cascades, a deep neural network reduces the noise originating from the acceleration. The post-cascades then conclude the reconstruction process. These consist solely of data-consistency steps resulting in a final estimate of the reconstructed image that is consistent with the acquired raw data.



5 Visualization of a single cascade within Deep Resolve Boost. A deep neural network leads to a denoised update of the image, while a data-consistency step ensures that the originally acquired raw data is represented in the final reconstruction. post-cascades then conclude the reconstruction process. These consist solely of data-consistency steps resulting in a final estimate of the reconstructed image that is consistent with the acquired raw data.

Deep Resolve Boost takes raw data from a reduced and therefore faster scan, and then applies an iterative process. A deep neural network is applied multiple times in an alternating fashion with data-consistency updates to generate the final output. The neural network leverages the benefits of physical models of MRI and data-driven models to achieve a high performance.

The technology comprises a fixed iterative reconstruction scheme implemented as a variational network framework, which is made up of multiple cascades (Fig. 4). Each cascade contains a data consistency step. This ensures that all the information encoded in the acquired data makes its way into the final image. This is then followed by a convolutional neural network-based regularization. The processing performed through this network results in the desired reduction of noise originating from the acceleration (Fig. 5).

Training and validation of the network are as important for the performance and robustness of a deep neural

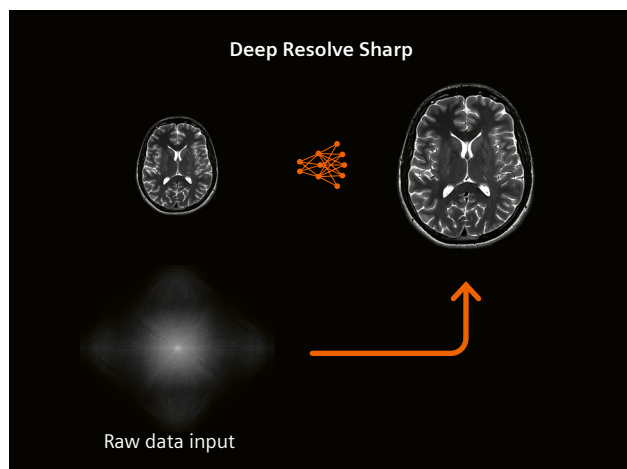
network as the architecture. More than 25,000 acquired slices were split into training ($\approx 90\%$) and validation ($\approx 10\%$) datasets. The acquisition covered a broad range of body parts, contrasts, fat suppression, orientations, and field strengths. A similar distribution of the data was used for both the training and the validation datasets. The wide-ranging and carefully curated nature of these training and validation datasets is an essential aspect that ensures the reliability and generalizability of Deep Resolve Boost.

The key to the success of Deep Resolve Boost lies in its ability to integrate raw data throughout the reconstruction process. Further enhancement of the image quality is achieved by additionally including coil-sensitivity maps estimated from calibration data as a preprocessing step not based on deep learning. Deep Resolve Boost offers three levels of denoising strength. These are achieved by adapting the weighting of the regularization through the neural network (Fig. 6).



6 Reconstructions of a T1 TSE acquisition of the knee with PAT 4 and SMS 2 using Deep Resolve Boost. (6A) Low denoising strength, (6B) medium denoising strength, (6C) high denoising strength.

Study ID: 1aaa4136



7 Visualization of the enhancement process within Deep Resolve Sharp. A deep neural network is employed in complex image space to increase the resolution and sharpness of the input image, leading to an increase in matrix size by a factor of 2 along both axes. A data-consistency step ensures that the acquired raw data is represented in the final reconstruction.

Deep Resolve Sharp

Deep Resolve Sharp is a novel image enhancement technology that uses a deep neural network to generate high-resolution images from low-resolution input data, resulting in substantially increased image sharpness and reduced Gibbs ringing. The technology is based on a convolutional neural network that operates on complex data and is trained on tens of thousands of pairs of low- and high-resolution data covering a wide range of anatomies.

Deep Resolve Sharp can raise image resolution by a factor of two along both in plane axes. Unlike conventional image enhancement techniques, Deep Resolve Sharp incorporates the acquired raw data directly into the enhancement process. This data-consistency step ensures robust results and correct representation of image contrast in the final output (Fig. 7).

Deep Resolve Sharp can increase the sharpness of reconstructed images without extending the acquisition time. It can also enable quicker scans. The phase resolution can be reduced in the acquisition, and Deep Resolve Sharp can recover the resolution in the reconstruction process.

Unlike conventional interpolation methods that expand k -space with zeros, the neural network at the heart of Deep Resolve Sharp enhances the image with meaningful information corresponding to the outer parts of k -space that represent higher frequencies.

Deep Resolve Swift Brain

Deep Resolve Swift Brain combines deep learning image reconstruction with a novel acquisition scheme to enable the acquisition of a brain imaging protocol with less than 2 minutes' scan time. To achieve this, the T2-, T2*-, and Dark Fluid-weighted contrasts are acquired with a deep learning accelerated multi-shot EPI (ms-EPI) sequence. A T1-weighted contrast is acquired with a deep learning-accelerated 2D GRE sequence. A Simultaneous Multi-Slice accelerated diffusion acquisition completes the Deep Resolve Swift Brain protocol.

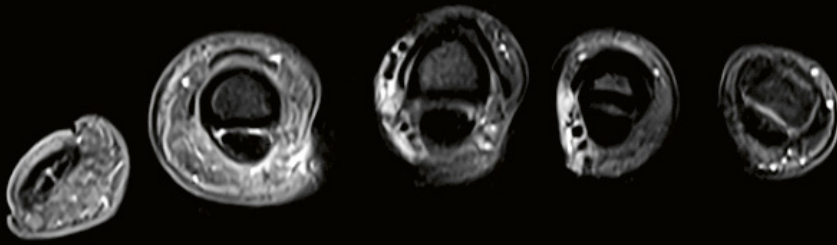
As EPI-based acquisitions are prone to distortion artifacts, an efficient static field correction is essential to achieve robust results. Deep Resolve Swift Brain employs a novel static field correction that drastically reduces distortion artifacts. The static field correction is a cornerstone of the ms-EPI acquisition, and delivers the required robust results.

This fast brain protocol is particularly useful when scanning patients who would otherwise struggle to cooperate for the duration of a conventional brain scan, which can take 10 minutes or more to complete.

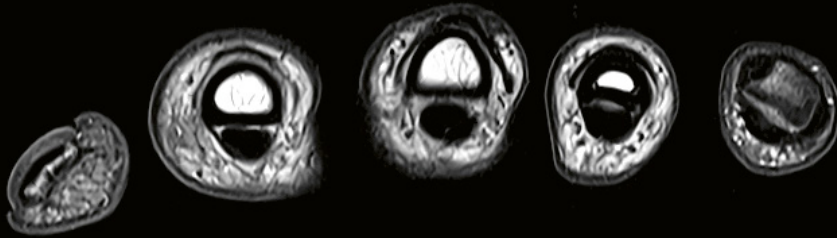
The best of both worlds

The introduction of deep learning reconstruction to routine clinical MRI is transformational in itself. However, its full potential lies in its combinability with conventional acceleration technology. While Compressed Sensing is an excellent acceleration tool for non-Cartesian acquisition and 3D data, its applicability to 2D Cartesian sampling is limited. With the introduction of Deep Resolve, and especially with the power of the neural networks in Deep Resolve Boost and Sharp, the basic reconstruction principle of Compressed Sensing can be combined with parallel imaging undersampling schemes. As 2D Cartesian sampling represents the majority of clinical MR acquisitions, this enhances the transformational character of Deep Resolve.

In addition to parallel imaging acceleration, Deep Resolve can be combined with Simultaneous Multi-Slice. This unique combination enables unmatched acceleration, especially in musculoskeletal and neurological applications. When a knee exam takes less than 2 minutes, MRI is approaching the point where the scan time is no longer the limiting factor for the examination (Figs. 8–14).



PD FS TSE, PAT 3, SMS 2,
Deep Resolve, $0.2 \times 0.2 \times 2.5 \text{ mm}^3$
TA 0:54 min



PD TSE, PAT 3, SMS 2,
Deep Resolve, $0.2 \times 0.2 \times 2.5 \text{ mm}^3$,
TA 0:40 min



Study ID: 1aaaa4302

PD FS TSE, PAT 3,
SMS 2, Deep Resolve,
 $0.3 \times 0.3 \times 2.5 \text{ mm}^3$,
TA 0:58 min

PD TSE, PAT 3,
SMS 2, Deep Resolve,
 $0.4 \times 0.4 \times 2.5 \text{ mm}^3$,
TA 1:05 min

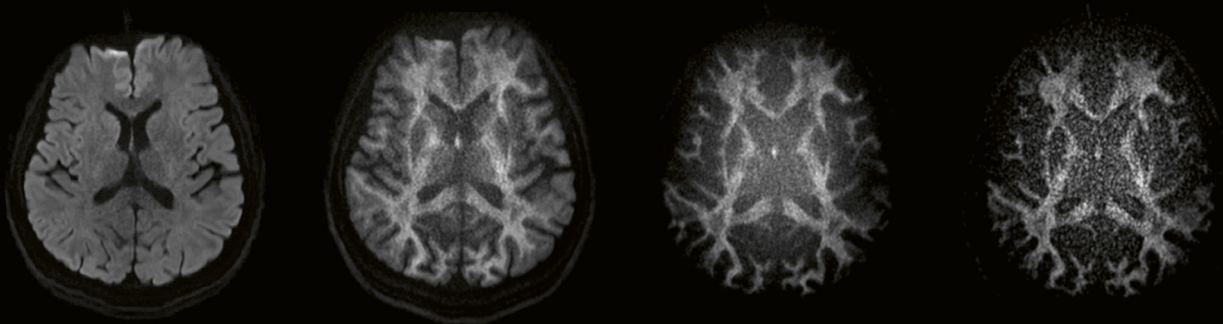
PD FS TSE, PAT 3,
Deep Resolve,
 $0.1 \times 0.1 \times 2.0 \text{ mm}^3$,
TA 0:42 min

PD TSE, PAT 3,
Deep Resolve,
 $0.1 \times 0.1 \times 2.0 \text{ mm}^3$,
TA 0:42 min

8 Finger imaging with Deep Resolve at 1.5T on MAGNETOM Sola.

PAT 2, Deep Resolve, $0.6 \times 0.6 \times 4.0 \text{ mm}^3$

Study ID: Zaaaa2641



B2000, TE = 73 ms

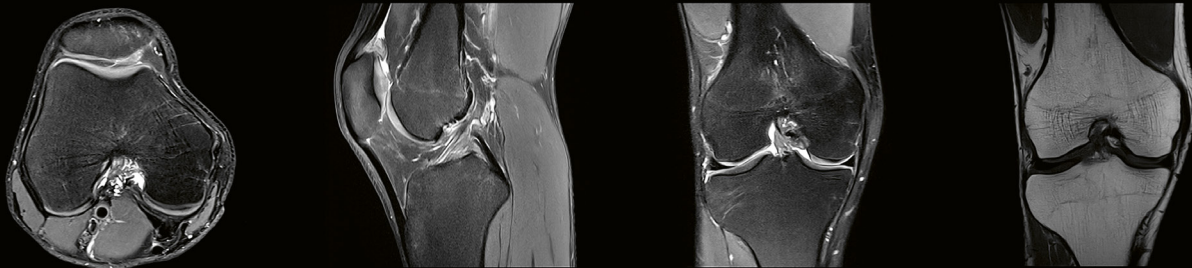
B52000, TE = 80 ms

B100000, TE = 87 ms

B160000, TE = 92 ms

9 Diffusion brain imaging with Deep Resolve at 3T on MAGNETOM Cima.X

Study ID: Zaaaa2296



PD TSE fs tra,
PAT 3, SMS 2, Deep Resolve,
 $0.2 \times 0.2 \times 3.0 \text{ mm}^3$,
TA 00:39 min

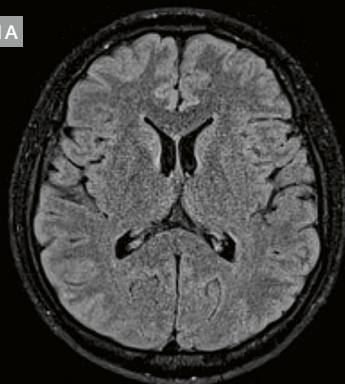
PD TSE fs sag,
PAT 3, SMS 2, Deep Resolve,
 $0.2 \times 0.2 \times 3.0 \text{ mm}^3$,
TA 00:36 min

PD TSE fs cor,
PAT 3, SMS 2, Deep Resolve,
 $0.2 \times 0.2 \times 3.0 \text{ mm}^3$,
TA 00:28 min

T1 TSE cor,
PAT 4, SMS 2, Deep Resolve,
 $0.2 \times 0.2 \times 3.0 \text{ mm}^3$,
TA 00:15 min

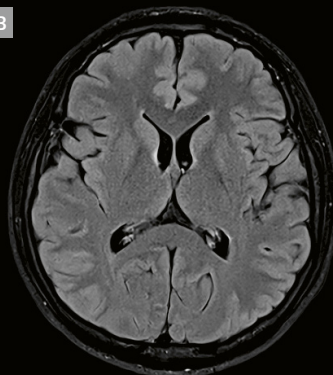
10 Complete knee exam in less than 2 minutes on a 3T MAGNETOM Vida.

11A



T2 FLAIR, PAT 3,
 $0.8 \times 0.8 \times 3.0 \text{ mm}^3$,
TA 1:48 min

11B



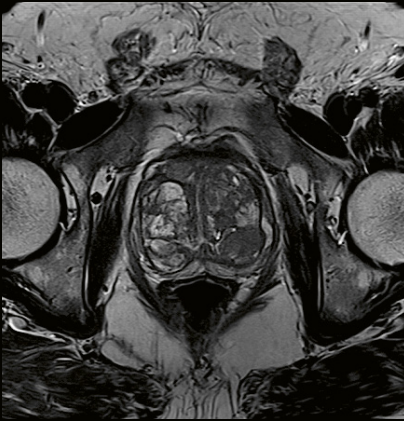
T2 FLAIR, PAT 3, Deep Resolve,
 $0.4 \times 0.4 \times 3.0 \text{ mm}^3$,
TA 1:48 min

11

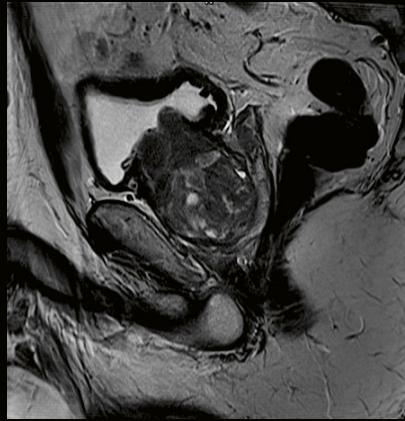
Brain imaging without (11A) and with (11B) Deep Resolve on MAGNETOM Sempra.

Study ID: 1aaaa4172

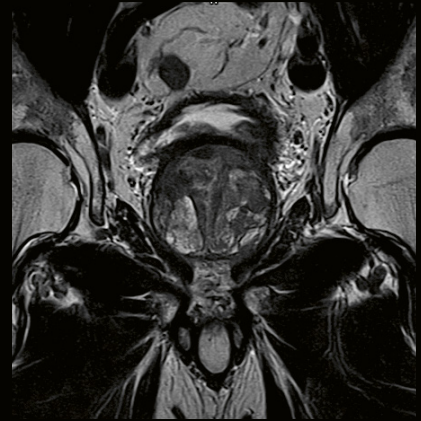
Study ID: 2aaaa2267



T2 TSE, PAT 4, Deep Resolve,
0.2 × 0.2 × 3.0 mm³,
TA 0:56 min



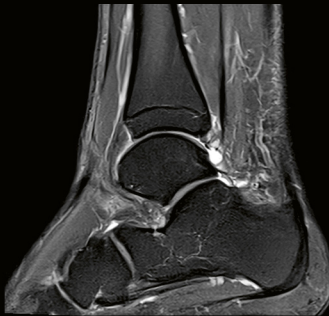
T2 TSE, PAT 4, Deep Resolve,
0.2 × 0.2 × 3.0 mm³,
TA 0:51 min



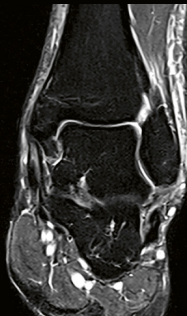
T2 TSE, PAT 4, Deep Resolve,
0.2 × 0.2 × 3.0 mm³,
TA 0:56 min

12 Prostate imaging with Deep Resolve at 3T on MAGNETOM Vida Fit.

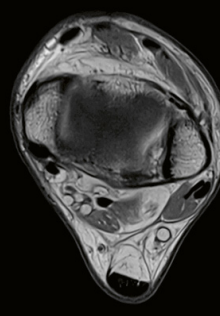
Study ID: 7aaaa0481



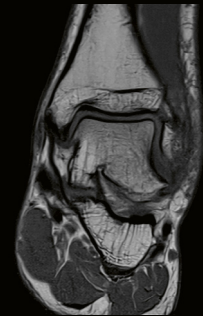
PD FS TSE, PAT 4,
Deep Resolve,
0.3 × 0.3 × 3.0 mm³,
TA 3:00 min



T2 STIR TSE, PAT 4,
Deep Resolve,
0.3 × 0.3 × 3.0 mm³,
TA 2:47 min



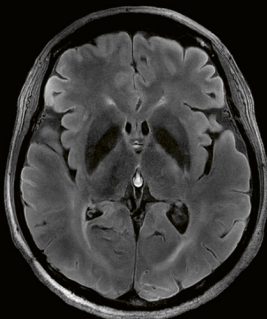
PD TSE, PAT 4,
Deep Resolve,
0.3 × 0.3 × 3.0 mm³,
TA 3:07 min



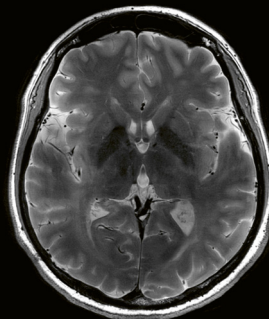
T1 TSE, PAT 4, SMS 2,
Deep Resolve,
0.3 × 0.3 × 3.0 mm³,
TA 2:29 min

13 Ankle imaging with Deep Resolve at 0.55T on MAGNETOM Free.Max.

Study ID: 1aaaa4172

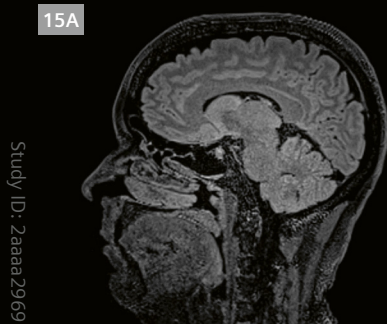


T2 FLAIR, PAT 3, Deep Resolve,
0.2 × 0.2 × 2.0 mm³,
TA 2:24 min

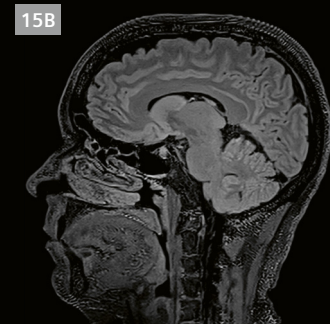


T2 TSE, PAT 4, Deep Resolve,
0.1 × 0.1 × 2.0 mm³,
TA 1:18 min

14 Brain imaging with Deep Resolve at 7T on MAGNETOM Terra.X.

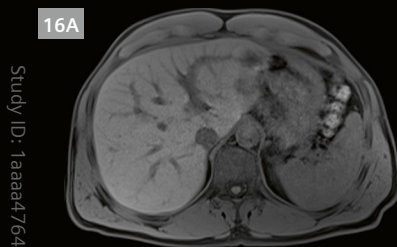


15A
T2 SPACE Dark Fluid,
CAIPI 6,
0.9 mm iso, TA 3:11 min

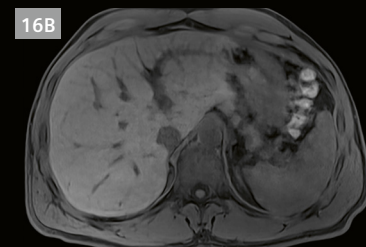


15B
T2 SPACE Dark Fluid,
CAIPI 6, Deep Resolve
0.45 mm iso, TA 3:11 min

15 T2 SPACE Dark Fluid of the head on a 3T MAGNETOM Vida, acquired and reconstructed without (15A) and with (15B) Deep Resolve. The reconstruction with Deep Resolve clearly displays improved SNR and improved sharpness. *Images courtesy of Jones Radiology, Adelaide, SA, Australia.*



16A
T1 VIBE fs,
CAIPI 4,
1.2 mm iso, TA 0:15 min

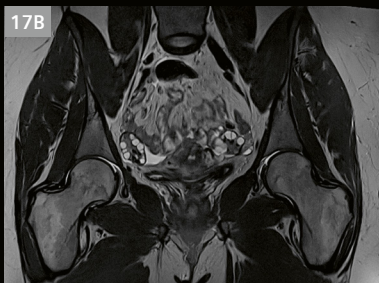


16B
T1 VIBE fs,
CAIPI 6, Deep Resolve,
0.6 mm iso, TA 0:06 min

16 T1 VIBE fs of the liver on a 1.5T MAGNETOM Sola, acquired and reconstructed without (16A) and with (16B) Deep Resolve. The reconstruction with Deep Resolve enables the acquisition with a CAIPIRINHA factor of 6, reducing the acquisition time to just 6 seconds while simultaneously increasing the SNR.



17A
T2 SPACE,
CAIPI 4,
0.9 × 0.9 × 1.0 mm³,
TA 5:30 min



17B
T2 SPACE,
CAIPI 6, Deep Resolve,
0.4 × 0.4 × 0.6 mm³,
TA 3:53 min

17 T2 SPACE of the female pelvis on 3T MAGNETOM Vida acquired and reconstructed without (17A) and with (17B) Deep Resolve. The reconstruction with Deep Resolve enables a reduction in scan time by about 30% and an increase in image sharpness. *Images courtesy of Benson Radiology, Ashford Specialist Centre, Ashford, SA, Australia.*

A new dimension in speed

There are now plans to expand Deep Resolve to 3D sequences, particularly VIBE and SPACE¹. The combined application of Deep Resolve Boost and Deep Resolve Sharp for these sequences is proving instrumental in achieving high-resolution 3D acquisitions in shorter scan times.

When applied to SPACE and VIBE, Deep Resolve Sharp operates in all three dimensions, which results in enhanced image sharpness and resolution, both in-plane and through-plane. This multi-dimensional operation can significantly improve the overall quality and clarity of the images (Figs. 15–17).

Furthermore, Deep Resolve for SPACE and VIBE can be effectively combined with CAIPIRINHA undersampling and acceleration. This unique combination has the potential to set new standards in image quality and efficiency for 3D MR imaging. By making the scans more time-efficient, Deep Resolve can pave the way for more widespread and routine use of high-resolution 3D imaging in clinical practice.

Conclusion

By bypassing the compromises inherent in conventional acceleration methods, Deep Resolve is transforming MRI with significantly shorter scan times and detailed depictions of intricate structures. The innovative technologies can help reduce long waiting times for MRI exams, improve the patient experience, and provide flexibility for including

¹Deep Resolve for SPACE and VIBE is currently under development and not commercially available. Its future availability cannot be ensured.

Contact

Nicolas Behl, Ph.D.
Siemens Healthineers
DI MR M&S SYS
Erlangen
Germany
nicolas.behl@siemens-healthineers.com



additional acquisitions that were previously omitted due to time constraints. Deep Resolve shows how AI can benefit healthcare by enabling greater precision and efficiency in MRI and by enhancing patient care.

Further reading

- 1 Gassenmaier S, Afat S, Nickel D, Mostapha M, Herrmann J, Othman AE. Deep learning-accelerated T2-weighted imaging of the prostate: Reduction of acquisition time and improvement of image quality. *Eur J Radiol.* 2021;137:109600.
- 2 Almansour H, Herrmann J, Gassenmaier S, Afat S, Jacoby J, Koerzdoerfer G, et al. Deep Learning Reconstruction for Accelerated Spine MRI: Prospective Analysis of Interchangeability. *Radiology.* 2023;306(3):e212922.
- 3 Kim EH, Choi MH, Lee YJ, Han D, Mostapha M, Nickel D. Deep learning-accelerated T2-weighted imaging of the prostate: Impact of further acceleration with lower spatial resolution on image quality. *Eur J Radiol.* 2021;145:110012.
- 4 Herrmann J, Keller G, Gassenmaier S, Nickel D, Koerzdoerfer G, Mostapha M, et al. Feasibility of an accelerated 2D-multi-contrast knee MRI protocol using deep-learning image reconstruction: a prospective intraindividual comparison with a standard MRI protocol. *Eur Radiol.* 2022;32(9):6215–6229.
- 5 Herrmann J, Wessling D, Nickel D, Arberet S, Almansour H, Afat C, et al. Comprehensive Clinical Evaluation of a Deep Learning-Accelerated, Single-Breath-Hold Abdominal HASTE at 1.5 T and 3 T. *Acad Radiol.* 2023;30(1):93–102.
- 6 Shanbhogue K, Tong A, Smereka P, Nickel D, Arberet S, Anthopoulos R, et al. Accelerated single-shot T2-weighted fat-suppressed (FS) MRI of the liver with deep learning-based image reconstruction: qualitative and quantitative comparison of image quality with conventional T2-weighted FS sequence. *Eur Radiol.* 2021;31(11):8447–8457.
- 7 Bae SH, Hwang J, Hong SS, Lee EJ, Jeong J, Benkert T, et al. Clinical feasibility of accelerated diffusion weighted imaging of the abdomen with deep learning reconstruction: Comparison with conventional diffusion weighted imaging. *Eur J Radiol.* 2022;154:110428.
- 8 Afat S, Herrmann J, Almansour H, Benkert T, Weiland E, Hölldobler T, et al. Acquisition time reduction of diffusion-weighted liver imaging using deep learning image reconstruction. *Diagn Interv Imaging.* 2023;104(4):178–184.
- 9 Lee EJ, Chang YW, Sung JK, Thomas B. Feasibility of deep learning k-space-to-image reconstruction for diffusion weighted imaging in patients with breast cancers: Focus on image quality and reduced scan time. *Eur J Radiol.* 2022;157:110608.